Multimode lasing in two-dimensional fully chaotic cavity lasers

Satoshi Sunada,[1,2] Takahisa Harayama,[1] and Kensuke S. Ikeda[2]
[1]*Department of Nonlinear Science, ATR Wave Engineering Laboratories, 2-2-2 Hikaridai Seika-cho, Soraku-gun, Kyoto 619-0288, Japan*
[2]*Department of Physics, Ritsumeikan University, 1-1-1 Noji-cho, Kusatsu, Shiga 525-0577, Japan*
(Received 21 October 2004; published 18 April 2005)

Multimode lasing in a fully chaotic cavity is investigated numerically by using a nonlinear dynamics model. We report a transition process from single-mode lasing to multimode lasing and reveal interactions among the lasing modes. In particular, both mode-pulling and mode-pushing interactions are shown to decrease the number of effective lasing modes. In addition, coexistence of different types of attractors of the final lasing states is numerically confirmed.

DOI: 10.1103/PhysRevE.71.046209 PACS number(s): 05.45.Mt, 42.55.Sa, 42.65.Sf, 42.65.Pc

I. INTRODUCTION

Two-dimensional (2D) microcavity lasers have attracted attention not only from the viewpoint of practical use but also from the perspective of fundamental physics, because they can exhibit new types of laser action owing to the morphological effects of the cavity shape. For example, microdisks can confine light efficiently due to total internal reflection and they have a high quality factor [1,2]. Lasing in whispering gallery modes has been realized in microdisk lasers. For application to optical systems, microdisk lasers have two problems: weak output power and no directionality. To solve the two problems, deformed microdisk cavity lasers have been proposed and directional emissions have been achieved [1,3,4].

Conventional theoretical approaches to 2D microcavity lasers, such as microdisk lasers, use ray dynamics, and the lasing modes have been described as linear resonance modes which correspond to the set of the ray trajectories satisfying the critical angle condition. In deformed microdisk lasers, it is also possible to describe the relation between the ray trajectories and linear resonance modes. The emission pattern of the deformed microdisk lasers can be explained by the linear resonance modes [4–7]. In fully chaotic cavity lasers, however, there are no ray trajectories satisfying the critical angle condition, and the resonance modes in the cavity do not have a simple description in terms of ray trajectories.

In a theoretical approach for fully chaotic cavity lasers, it is important to take into account nonlinear interaction between the light field and an active medium [8]. A nonlinear dynamical treatment of 2D microcavity lasers has been carried out with the Schrödinger-Bloch model. This model consists of the (classical) Maxwell equations and the optical Bloch equations which describe time-evolution of the active medium. So far, single-mode lasing and two-mode lasing in fully chaotic cavities have been studied by using the dynamics model. For example, in Ref. [9], it is shown that single-mode lasing can be well explained by one resonance mode. In Ref. [10], nonlinear interaction between two modes is studied, and it is shown that locking between two resonance modes of different symmetry classes leads to an asymmetric lasing pattern. However, interaction among more than two lasing modes has never been studied in detail. Since laser action in real experiments typically occurs in multimode lasing, it is important to study interactions among many modes.

Recently, a semiconductor laser diode with the shape of a stadium has actually been fabricated, and the lasing in the cavity has been demonstrated [11]. We note that the ray trajectories show chaos in a stadium cavity [12]. The emissions in the far-field have been explained by a ray dynamics model, which gives a distribution of the emission angles of rays which are confined inside the cavity for a long time and finally violate the critical angle condition. However, the detailed physics of the lasing are not yet understood.

In this paper, we numerically investigate multimode lasing and the dynamics in a stadium-shaped cavity by using the Schrödinger-Bloch model. Although this model is simplified compared to a prior theoretical model that describes the dynamics of quantum operators of the light field and semiconductor material in detail [13], the Schrödinger-Bloch model can qualitatively reproduce a phenomenon observed in a real experiment, as shown in Ref. [10]. We obtained the following results by using this model: (i) In the multimode lasing state, not only mode-pulling interaction but also mode-pushing interaction occurs. It is shown that the mode-pushing interaction reduces the number of lasing modes. (ii) There exist multiattractors of the final lasing states for sufficiently high pumping power. That is, the final lasing state depends on the initial state of the light field.

II. NONLINEAR DYNAMICS MODEL

First let us explain the Schrödinger-Bloch model. The dynamics of the slowly varying envelope of the electric field $\tilde{E}$, the polarization field $\tilde{\rho}$, and the population inversion component W is described by this model when the 2D microcavity is confined in a waveguide which is wide in the xy directions, and the refractive index suddenly changes on the edge of the cavity

$$\frac{\partial \tilde{E}}{\partial t} = \frac{i}{2}\left(\nabla_{xy}^2 + \frac{n^2}{n_{\text{in}}^2}\right)\tilde{E} - \alpha_L(x,y)\tilde{E} + \frac{2\pi N\kappa\hbar}{\epsilon}\tilde{\rho}, \tag{1}$$

$$\frac{\partial \tilde{\rho}}{\partial t} = -i\Delta_0\tilde{\rho} - \tilde{\gamma}_\perp\tilde{\rho} + \tilde{\kappa}W\tilde{E}, \tag{2}$$

$$\frac{\partial W}{\partial t} = -\tilde{\gamma}_{\parallel}(W - W_{\infty}) - 2\tilde{\kappa}(\tilde{E}\tilde{\rho}^{*} + \tilde{E}^{*}\tilde{\rho}), \tag{3}$$

where space and time are made dimensionless by the scale transformation $(n_{\mathrm{in}}\omega_s x/c, n_{\mathrm{in}}\omega_s y/c) \rightarrow (x,y)$ and $t\omega_s \rightarrow t$, respectively. In the above, ω_s is the oscillation frequency of a light field that is slightly different from the transition frequency ω_0 of the two-level medium, and the refractive index n equals n_{in} inside the cavity and n_{out} outside the cavity, and $\alpha_L(x,y)$ is the linear absorption coefficient, which is the constant α_L inside the cavity and zero outside the cavity. The two (dimensionless) relaxation parameters $\tilde{\gamma}_{\perp}$ and $\tilde{\gamma}_{\parallel}$, are the transversal relaxation rate and the longitudinal relaxation rate, respectively, and W_{∞} is the external pumping parameter. $\tilde{\kappa}$ is the dimensionless coupling strength, and $\Delta_0 = \omega_0/\omega_s - 1$. Δ_0 plays the role of the gain center.

A stadium cavity consists of two half circles of the radius $R = 98/\sqrt{2}$ and two flat lines of the length $2R$. We set the refractive index inside and outside the stadium to $n_{\mathrm{in}} = 2$ and $n_{\mathrm{out}} = 1$, respectively. The other parameters are given as follows: $\tilde{\gamma}_{\parallel} = 0.003$, $\tilde{\gamma}_{\perp} = 0.006$, $\epsilon = 4.0$, $\alpha_L = 0.004$, $N\kappa\hbar\omega_0 = 1.0$, $\tilde{\kappa} = 0.5$, and $\Delta_0 = -0.03$. In this model, all of the quantities are made dimensionless. If we were to assume the wavelength of the lasing mode to be 0.8 μm, the flat line of the length of the stadium would be 2.21 μm.

By neglecting the absorption term and the polarization term and assuming the envelope of electric field $\tilde{E}$ oscillates as $\tilde{E} = \psi e^{-i\Delta t}$ in the approximated Maxwell equation (1), the eigenvalue (resonance) Δ and the wave function ψ corresponding to the resonance can be obtained as follows:

$$\left[\nabla_{xy}^2 + \left(2\Delta + \frac{n^2}{n_{\mathrm{in}}^2}\right)\right]\psi = 0, \tag{4}$$

where the Δ is a complex value because the cavity is an open system. The Δ and ψ can be calculated by the extended boundary element method [14]. We show the resonances and the wave functions of the stadium cavity of the $R = 98/\sqrt{2}$ in Fig. 1. The real and imaginary parts of the Δ represent, respectively, the resonant frequency and decay rate of the resonance mode.

It is important to note that the stadium cavity is symmetric with respect to the x and y axes. The resonances are divided into four symmetry classes $\psi_{ab}(-x,y) = a\psi_{ab}(x,y)$ and $\psi_{ab}(x,-y) = b\psi_{ab}(x,y)$ with the parities $a \in \{+,-\}$ and $b \in \{+,-\}$. In the labels of the resonances shown in Fig. 1, "e" and "o," respectively denote the $+$(even) and $-$(odd) parities of the resonance wave functions.

The lasing possibility of a resonance mode can be predicted by linear analysis of the nonlinear dynamics model (1)–(3). In a linear description in which the nonlinear term of Eqs. (1)–(3) is neglected, one can calculate the lasing gain which is a Lorentzian function in frequency space and maximum for a resonant frequency $\mathrm{Re}\,\Delta = \Delta_0$. Whether a mode can lase depends on total lasing gain. The total lasing gain is given as the first-order correction of the imaginary part of the resonance frequency due to the presence of the linear absorption and the active medium [9]. When a mode has a positive total lasing gain, that is, the lasing gain exceeds the total loss

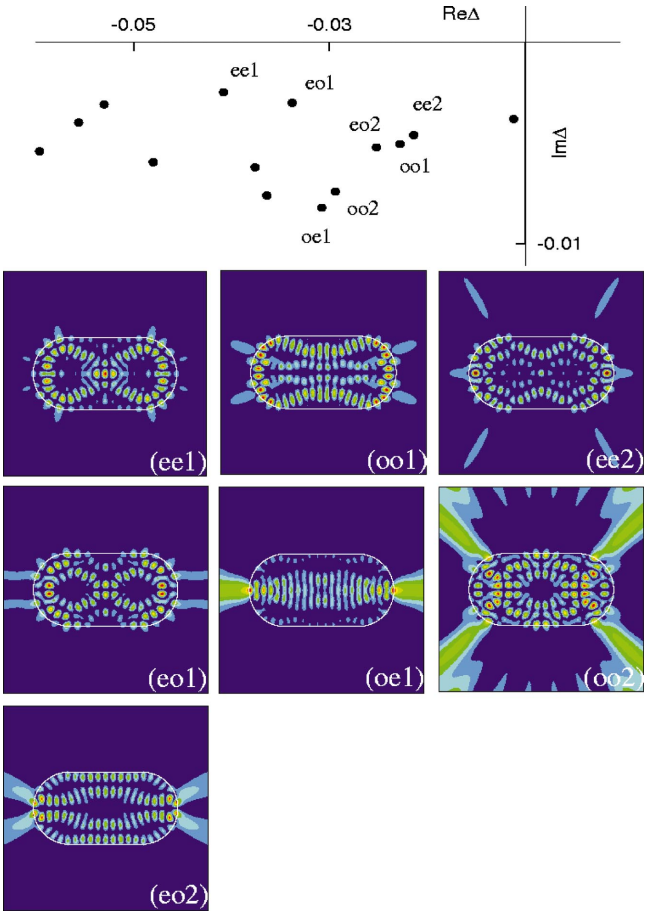

FIG. 1. (Color) The resonances and the corresponding wave functions of a stadium cavity.

term, the mode has a possibility to lase. However, this description is correct only when the light intensity is low enough. Moreover, when many modes have a positive total lasing gain, the lasing condition based on the linear analysis is less effective at explaining the lasing states. Therefore, we carry out numerical simulations on the Schrödinger-Bloch equations to investigate multimode lasing.

III. RESULTS OF NUMERICAL SIMULATIONS

A. Multimode lasing

Here, we explain a transition process from single-mode lasing to multimode lasing when the pumping power W_{∞} is increased. For $W_{\infty} = 0.15 \times 10^{-3}$, only the mode *eo*1 shown in Fig. 1 has a positive total lasing gain, because the frequency of mode *eo*1 is close to the gain center, and the decay rate is small. In this case, even a mode with the smallest decay rate (i.e., mode *ee*1) cannot obtain any lasing gain, because its frequency is far from the gain center $\Delta_0 = -0.03$. Therefore, only mode *eo*1 can lase. This can be confirmed by the optical spectrum in the stationary regime and the wave function of the final lasing state, as shown in Fig. 2. The optical spectrum has only one peak corresponding to the frequency of mode *eo*1. In addition, one can see that the lasing pattern of the final lasing state shown in Fig. 2 corresponds well to that of mode *eo*1 shown in Fig. 1.

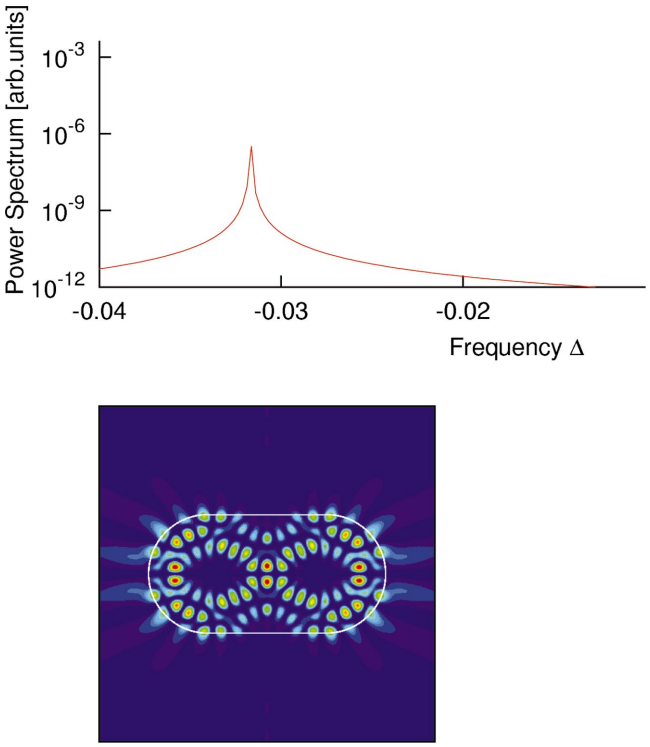

FIG. 2. (Color) The optical spectrum and the wave function when the pumping power $W_\infty = 0.15 \times 10^{-3}$.

For $W_\infty = 0.25 \times 10^{-3}$, mode $eo2$ can also have positive total lasing gain and starts to lase. Mode $eo2$ interacts with mode $eo1$, and the optical spectrum has two main peaks corresponding to the frequencies of the two modes $eo1$ and $eo2$ and the harmonics of the two modes. For $W_\infty = 0.3 \times 10^{-3}$, the mode $oe1$ starts to lase. In this lasing state, mode $oe1$ interacts with the two modes $eo1$ and $eo2$. In Fig. 3, we show the optical spectrum in this lasing state and the wave functions of the lasing modes corresponding to the peaks of the optical spectrum. The wave function of the lasing modes with the frequency Δ is given as follows:

$$\tilde{E}(\Delta, r) = \lim_{T \to \infty} \frac{1}{T} \int_0^T \tilde{E}(t, \boldsymbol{r}) e^{i\Delta t} dt. \tag{5}$$

In actual calculations, we set $T = 104857.6$, and the value of the frequency Δ is determined from the peaks of the optical spectrum. Comparing the lower panel in Fig. 3 with that in Fig. 1, one can see that the lasing mode for peak (b) corresponds to the resonance mode $eo2$. On the other hand, the lasing mode for peak (a) is slightly asymmetric with respect to the x and y axes, and does not correspond to any resonance modes. This asymmetricity can be explained as follows. Since the difference in the frequencies of the two modes $eo1$ and $oe1$ is small, the frequencies of two modes $eo1$ and $oe1$ are easily locked so that the difference in the frequencies becomes zero. Superposition of the two different parity modes with the same frequency yields an asymmetric pattern [10]. Moreover, the locked state of the two modes $eo1$ and $oe1$ interacts with mode $eo2$. Therefore, the optical

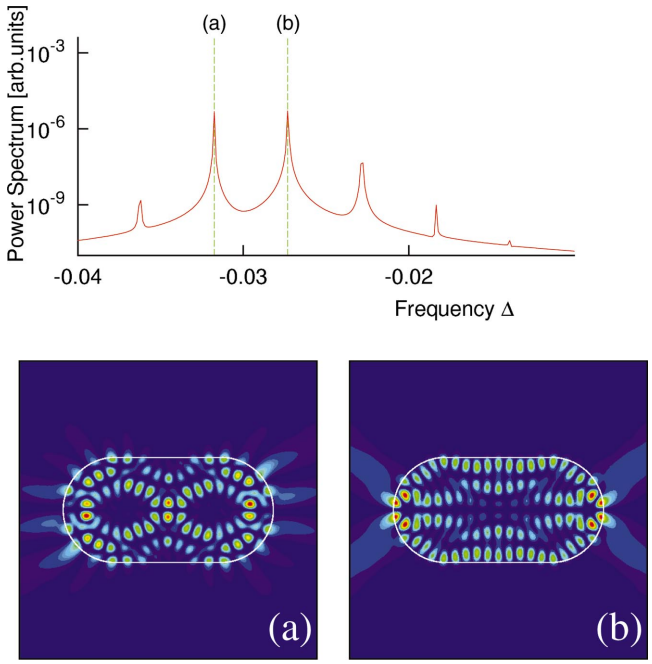

FIG. 3. (Color) The optical spectrum when the pumping power $W_\infty = 0.3 \times 10^{-3}$. The wave functions of the lasing modes correspond to the peaks (a) and (b), respectively.

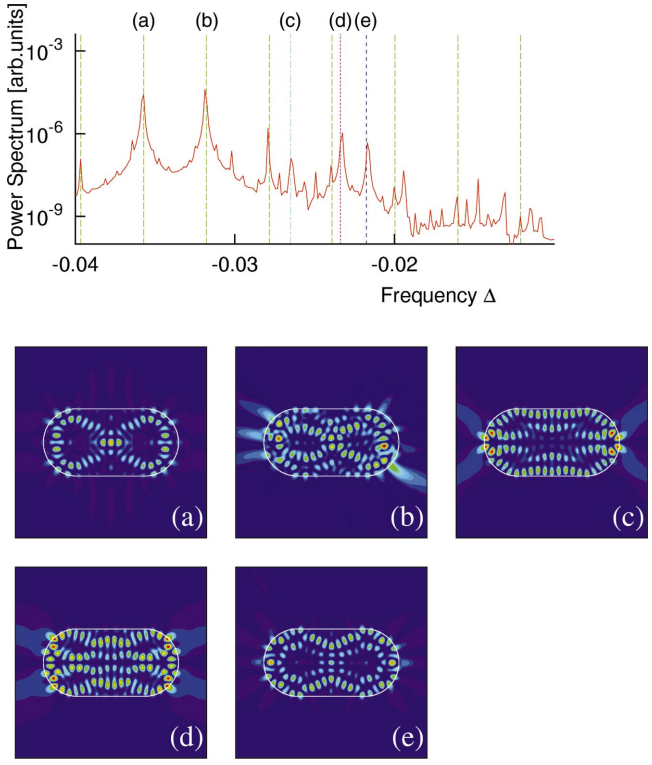

FIG. 4. (Color) The optical spectrum when the pumping power $W_\infty = 1.6 \times 10^{-3}$. The wave functions of the lasing modes correspond to the peaks (a)–(e). The wave functions of the peaks (a) (green line), (c) (blue line), (d) (red line), and (e) (purple line) correspond to those of resonance modes $ee1$, $eo2$, $oo1$, and $ee2$, respectively, while the wave function of (b) (green line) is the locked state of modes $eo1$, $oe1$, and $oo2$. The other peaks shown by green line are the harmonics of mode (a) and (b).

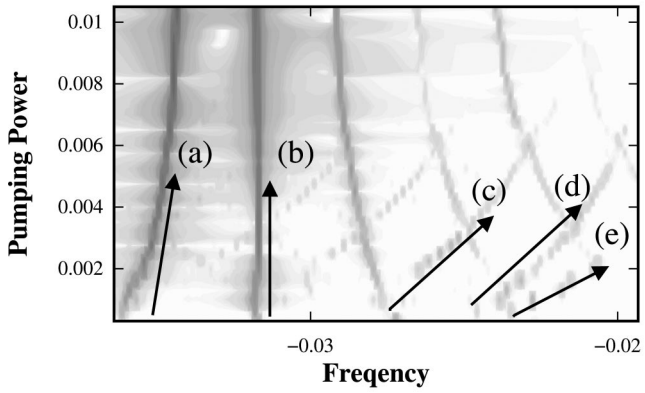

FIG. 5. The W_∞ dependence of the position of the peaks in the optical spectrum. The peaks labeled by letters (a)–(f) correspond to the lasing modes in Fig. 4. The lasing modes labeled by (a), (c), (d), and (e) correspond to the resonance modes *ee*1, *eo*2, *oo*1, and *ee*2 in Fig. 1, respectively. The mode labeled (b) corresponds to the locked state of the three resonance modes *eo*1, *oe*1, and *oo*2. In this figure, since the difference in the frequencies among modes *eo*1, *oe*1, and *oo*2 is small, one cannot see the locking process of the three modes. The peaks (a) and (b) are pulled toward each other as the pumping power increases. The peaks indicated by (c), (d), and (e) are shifted and leave the gain center. The peak (e) and a harmonic of modes (a) and (b) are locked for $W_\infty = 2.25 \times 10^{-3}$. On the other hand, the peaks (c) and (d) are not locked with any harmonic. The intensities of the two lasing modes (c) and (d) decrease as the two modes leave the gain center, and disappear for $W_\infty = 8.0 \times 10^{-3}$.

spectrum also shows the harmonics of the locked state and mode *eo*1.

Figure 4 shows the optical spectrum for $W_\infty = 1.6 \times 10^{-3}$ where the peaks correspond to mode *eo*1, *oe*1, *eo*2, *ee*1, *ee*2, *oo*1, and *oo*2. In this figure, it is observed that the lasing modes for the peaks of (a), (c), (d), and (e) correspond to the resonance modes *ee*1, *eo*2, *oo*1, and *ee*2, respectively. On the other hand, one can see strong asymmetricity in the lasing mode (b). This can be explained by the locking of three different parity modes *eo*1, *oe*1, and *oo*2, because the frequency of mode *oo*2 is close to that of the locked state of *eo*1 and *oe*1. In this multimode lasing, since a mode interacts with many modes, many harmonics are observed in the optical spectrum.

For $W_\infty > 1.6 \times 10^{-3}$, all resonance modes shown in Fig. 1 can have positive total lasing gain. However, only some modes can lase. This is caused by mode competition for obtaining lasing gain. Only a limited number of modes can contribute to the lasing state even in the case of strong pumping.

In Fig. 5, we show the W_∞ dependence of the position of the peaks in the optical spectrum. The frequency shifts in Fig. 5 are caused by two types of mode interaction: mode pulling and pushing. The labels (a)–(f) in Fig. 5 correspond to the lasing modes shown in Fig. 4. In Fig. 5, modes (a) and (b) pull each other, and the harmonics are also shifted according to mode-pulling interaction between modes (a) and (b), while the shifts of the three peaks (c), (d), and (e) are caused in the direction that leaves the gain center $\Delta_0 = -0.03$.

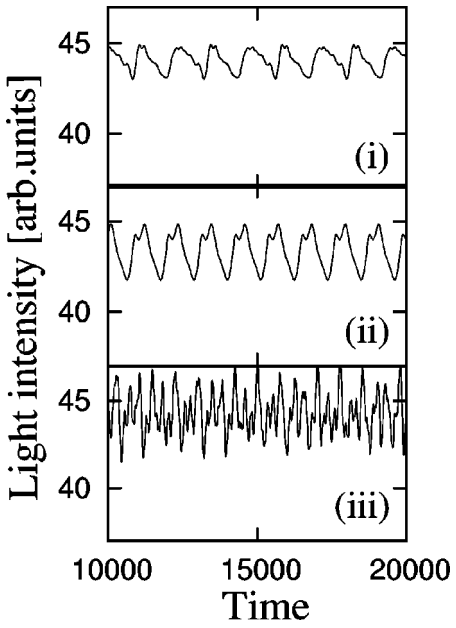

FIG. 6. The light intensity inside the cavity vs time of type I (i), type II (ii), and type III (iii), when the pumping power $W_\infty = 10 \times 10^{-3}$.

One can see that the peak (e) approaches a harmonic of modes (a) and (b) and finally at around $W_\infty = 2.25 \times 10^{-3}$ the two peaks merge. On the other hand, the peaks (c) and (d) are not locked and are pushed from the gain center. When a mode is separated from the gain center, it obtains less lasing gain. As can be seen in Fig. 5, the intensity of the pushed modes decreases and these modes disappear for $W_\infty = 8.0 \times 10^{-3}$. This result shows that the mode-pushing interactions have the effect of mode selections.

B. Multiattractors

The final lasing state discussed above mainly consists of modes *eo*1, *oe*1, *oo*2, *ee*1, and *ee*2. The three modes *eo*1, *oe*1, and *oo*2 are locked, and mode *ee*2 is locked with the harmonic of the locked state and mode *ee*1. Therefore, this final lasing state is a limit cycle attractor formed by the interaction among the lasing modes, whose time evolution is shown in Fig. 6(i), and the time-averaged lasing pattern becomes asymmetric with respect to the *x* and *y* axes due to the locking of many modes, as shown in Fig. 7(i).

When the pumping power is weak, all initial states of the light field converge to the same attractor by the time evolution. However, we found two attractors in addition to this attractor in the case of strong pumping power. That is, the final lasing state depends on the initial state of the light field. We call the first attractor type I, and the other two attractors type II and type III.

The type-II attractor is a lasing state which consists mainly of modes *ee*1, *eo*1, *eo*2, *oo*1, and *oo*2. The attractor can be observed for $W_\infty > 4.22 \times 10^{-3}$. As the pumping power increases, the mode-pushing interaction acts on modes *eo*2 and *oo*1. As a result, the intensities of the two modes decrease, and the two modes finally disappear, because the

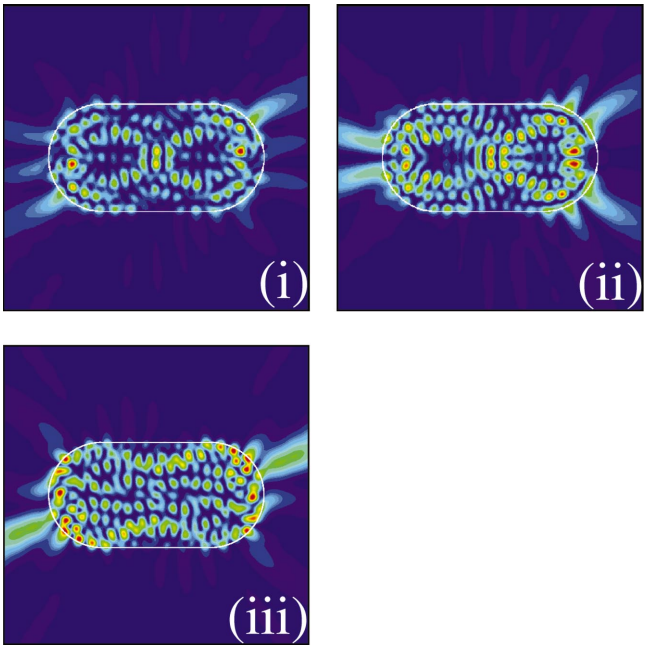

FIG. 7. (Color) The time-averaged wave functions of type I (i), type II (ii), and type III (iii), when the pumping power $W_\infty = 10 \times 10^{-3}$.

pushed modes are separated from the gain center and lose in the mode competition. For $W_\infty = 10 \times 10^{-3}$, the attractor becomes another limit cycle, as shown in Fig. 6(ii), where the locking mode of *eo*1 and *oo*2 exists and the locking mode interacts with *ee*1. The time-averaged lasing pattern becomes asymmetric with respect to the *y* axis due to the locking of the two modes *eo*1 and *oo*2, as shown in Fig. 7(ii).

The type-III attractor consists mainly of modes *ee*1, *eo*1 and the locked state of *oo*1 and *ee*2. In the optical spectrum of this lasing state, although many modes are observed compared with the above two attractors, the amplitudes of the other modes except for modes *ee*1, *eo*1 and the locked state are small. The intensity changes in a very intricate way, as shown in Fig. 6(iii), suggesting that this attractor might be chaotic. This attractor can be observed for $W_\infty > 6.0 \times 10^{-3}$. The time-averaged lasing pattern becomes asymmetric with respect to the *x* and *y* axes due to the locking of the two modes *ee*2 and *oo*1, as shown in Fig. 7(iii).

IV. SUMMARY AND DISCUSSIONS

In this paper, we have investigated multimode lasing in a stadium-shaped cavity laser by employing the Shrödinger-Bloch model. Various mode interactions have been observed. We showed that multimode lasing states do not necessarily consist of all resonance modes with positive total lasing gain; some modes winning in the mode competition can lase. When the pumping power increases and mode couplings become strong, both mode-pulling and mode-pushing interactions occur in the lasing state. The mode-pushing interaction suppresses some modes by separating the lasing frequencies from the gain center, while the mode-locking interaction unifies two or three lasing modes to form one locked mode. Consequently, both interactions work so that the number of effective lasing modes decreases.

We have carried out similar analysis also for a circular cavity [15]. For the circular cavity, it has been never observed that the number of lasing modes decreases due to the effects of the mode selection and the integration of mode even for high pumping power. We expect that the difference can be explained by the difference in mode-coupling structure between nonchaotic cavity lasers and fully chaotic cavity lasers.

We have also shown the existence of multiattractors of the final lasing states. The number of attractors depends on the pumping power. We numerically confirmed two attractors for $4.22 \times 10^{-3} < W_\infty < 6.0 \times 10^{-3}$ and three attractors for $6.0 \times 10^{-3} < W_\infty$. Each attractor consists of different lasing modes. Thus, the time-averaged lasing patterns of the attractors are different to each other. The existence of multiattractors might be used to switch the emission patterns.

ACKNOWLEDGMENTS

The work at ATR was supported in part by the National Institute of Information and Communication Technology of Japan.

[1] *Optical Processes in Microcavities*, edited by R. K. Chang and A. J. Campillo (World Scientific, Singapore, 1996).
[2] S. L. McCall, A. F. J. Levi, R. E. Slusher, S. J. Pearton, and R. A. Logan, Appl. Phys. Lett. **60**, 289 (1992).
[3] J. U. Nöckel and A. D. Stone, Nature (London) **385**, 45 (1997).
[4] C. Gmachl, F. Capasso, E. E. Narimanov, J. U. Nöckel, A. D. Stone, J. Faist, D. L. Sivco, and A. Y. Cho, Science **280**, 1556 (1998).
[5] C. Gmachl, E. E. Narimanov, F. Capasso, J. N. Baillargeon, and A. Y. Cho, Opt. Lett. **27**, 824 (2002).
[6] S. B. Lee, J. H. Lee, J. S. Chang, H. J. Moon, S. W. Kim, and K. An, Phys. Rev. Lett. **88**, 033903 (2002).
[7] J. U. Nöckel, A. D. Stone, and R. K. Chang, Opt. Lett. **21**, 1693 (1994).
[8] T. Harayama, P. Davis, and K. S. Ikeda, Prog. Theor. Phys. Suppl. **139**, 363 (2000).
[9] T. Harayama, P. Davis, and K. S. Ikeda, Phys. Rev. Lett. **90**, 063901 (2003).
[10] T. Harayama, T. Fukushima, S. Sunada, and K. S. Ikeda, Phys. Rev. Lett. **91**, 073903 (2003).
[11] T. Fukushima and T. Harayama, IEEE J. Quantum Electron. **10**, 1039 (2004).
[12] L. A. Bunimovich, Commun. Math. Phys. **65**, 295 (1979).
[13] H. F. Hofmann and O. Hess, Phys. Rev. A **59**, 2342 (1999).
[14] J. Wiersig, J. Opt. A, Pure Appl. Opt. **5**, 53 (2003).
[15] S. Sunada, T. Harayama, and K. S. Ikeda (unpublished).